
Micro-Raman spectroscopic investigation of dental calcified tissues

K. A. Schulze, M. Balooch, G. Balooch, G. W. Marshall, S. J. Marshall

Department of Preventive and Restorative Dental Sciences, Division of Biomaterials and Bioengineering, University of California San Francisco, San Francisco, California 94143-0758

Received 6 January 2003; revised 10 November 2003; accepted 14 November 2003

Published online 25 February 2004 in Wiley InterScience (www.interscience.wiley.com). DOI: 10.1002/jbm.a.20130

Abstract: The purpose of this study was to determine if dental calcified junctions (DEJs/CDJs) in human teeth contain different compositional phases compared to the adjacent dental calcified tissues. Peak positions and intensities were determined from micro-Raman spectra for PO_4^{3-} and the C—H modes and compared among the mineralized tissues and their junctions. Values of width were determined from the intersections of intensity regression lines through the junctions and in the adjacent tissues. The peaks were measured in 1- μm steps along a 100- μm line across the junction. High-resolution analysis revealed that PO_4^{3-} band peaks for dentin, the DEJ, enamel, the CDJ, and cementum were at the same position (959 cm^{-1}), while for the C—H stretching mode a significant shift of 4.6 cm^{-1} was found

between enamel, the DEJ, and dentin. The mean width of the DEJ was $7.6 (\pm 2.8)\ \mu\text{m}$ using the PO_4^{3-} band and $8.6 (\pm 3.6)\ \mu\text{m}$ using the C—H stretching mode. Across the DEJ, the mineral content monotonically decreased from enamel to dentin while the organic component monotonically increased. The DEJ width was in agreement with prior nanoindentation studies. No width estimate was possible for the CDJ because the compositional differences between cementum and dentin were small. © 2004 Wiley Periodicals, Inc. *J Biomed Mater Res* 69A: 286–293, 2004

Key words: Raman spectroscopy; dentin–enamel junction; cementum–dentin junction; tooth; phosphate band; C—H stretching mode

INTRODUCTION

Dentin, enamel, and cementum formation involves a remarkable orchestration of complex molecular and cellular events that culminate in uniquely structured tissues joined at distinctive interfaces. The dentino–enamel junction (DEJ) is the natural junction that unites the dentin with the enamel in a functionally graded region.^{1–4} It has been found that the DEJ is resistant to acid attacks⁵ as well as to mechanical forces such as crack propagation.^{2,3,6} The DEJ has a unique structure with at least three levels of microstructure.^{7–9} The scallops house microscallops that contain finer nanoscale structures.^{2,10} The scallops and the presence of a smooth gradient of mechanical properties at the junction are believed to contribute to an important toughening mechanism that reduces stress concentrations. This gradation of properties is initiated by a biomineralization process starting from the

DEJ in both directions.^{3,8,11} The DEJ is the junction of coronal dentin and enamel and is formed by the secretion of dentin on one side and of enamel on the other side. The nature of the cemento–dentin junction (CDJ) is controversial and it is not clear whether it is a form of dentin, cementum, or a tissue in its own right. This layer has been called “interzonal layer,”¹² “intermediate layer of cementum,”¹³ and “intermediate cementum.”¹⁴ Studies on the CDJ have been mostly of histological nature. Only few physical properties of cementum have been investigated.¹⁵ From the CDJ dentin is formed internally and cementum externally. However, the structure of the CDJ remains unclear.

Several mechanical properties studies^{1,2,16–18} as well as conventional morphological studies^{19,20} have been conducted on the DEJ and the CDJ, but these techniques lack the ability to obtain chemically related information. Raman microspectroscopy produces the capability to characterize the spatial distributions of organic compounds and inorganic compounds with spatial resolution of about $1\ \mu\text{m}$.²¹ Previous studies have used vibrational analysis to characterize interfaces between dentin and resin or enamel and resin to evaluate bonding to the altered dentin/enamel surface.^{21–23} The enamel Raman spectrum is dominated

Correspondence to: G. W. Marshall; e-mail: graymar@itsa.ucsf.edu

Contract grant sponsor: NIH/NIDCR; contract grant numbers: R01 DE 13029, P01DE09859

by bands that can be attributed to the mineral apatite at 591, 961, and 1071 cm^{-1} . The dentin and cementum spectra indicate the presence of much larger proportions of organic material. The C—H stretching bands at 2940 and 2880 cm^{-1} are more intense, and amide I and III bands at 1670 and 1243 cm^{-1} have been identified. These bands, which correlate with those found in the Fourier transform Raman spectra for bone, may indicate a similar protein composition in the two materials.²⁴

The first aim of this study was to determine if the DEJ is a different phase than the adjacent substrates. Therefore, the chemical composition of these substrates was analyzed using micro-Raman spectroscopy. The intensity values of the spectra obtained from the inorganic component, represented by PO_4^{3-} band peaks (apatite), as well as the spectra obtained from the organic component, represented by C—H stretching mode (collagen), reveal this information. Shift analysis of the peaks in these spectra allows the chemical contents of the tissues to be differentiated. The hypothesis tested was that the DEJ and CDJ consist of phases with different composition than the adjacent tissues. The second aim was to determine the width of the DEJ using phosphate and C—H band intensity changes.

MATERIALS AND METHODS

Sample preparation

Extracted sound human third molars, from subjects requiring such extractions as part of their dental treatment, were selected for this study. These procedures have been conducted according to an informed consent protocol that has been approved by the UCSF Institutional Committee on Human Research. Three teeth were gamma radiated²⁵ and stored at 4°C in deionized water until prepared. Sagittal buccolingual sections were prepared to obtain slabs of 1-mm thickness, containing enamel, the DEJ, dentin, the CDJ, and cementum. The specimens were polished with a series of SiO_2 papers and on polishing cloths with different diamond suspensions through 0.25 μm . Ultrasonic treatments in deionized water for 60 s were used between polishing stages to clean the surface and remove the remnant smear layer.

Raman microspectroscopy

The Raman spectra were recorded on a HR 800 Raman spectrophotometer (Jobin Yvon, Horiba, France) using monochromatic radiation emitted by a He—Ne laser (632.8 nm), operating at 20 mW of power, before entrance optics. Laser scanning imaging resolution was about 0.5 μm . All measurements were made systematically under the same conditions, utilizing $\approx 1 \mu\text{m}$ depth of laser penetration (“hole

adjustment setting”). A computer-controlled translation stage was used to move the specimen under the laser beam in 1- μm increments.

The spectral processing of the data included the subtraction of the luminescence background from the total spectra and deconvoluting the peaks by curve fitting of the Raman peaks.

Compositional analysis of mineralized dental hard tissue

For the high-resolution analysis three samples were selected to obtain spectra with a 100 \times microscope objective with a small confocal hole (to increase spatial resolution) and slit (to improve spectral resolution). The locations were in dentin, 100 μm from the DEJ; at the DEJ; in enamel, 100 μm from the DEJ; at the CDJ; and in cementum, 50 μm from the CDJ. The latter measurement was only 50 μm from the CDJ because the cementum is thin in some teeth. Figure 1 is a schematic showing a tooth section and locations where Raman measurements were made on each tooth. All spectra were obtained with an acquisition time of 600 s for the phosphate band at $\approx 960 \text{ cm}^{-1}$ and for the C—H stretching mode at $\approx 2937 \text{ cm}^{-1}$. The C—H stretching mode was chosen as an indicator for organic content because the luminescence at the 2900- cm^{-1} band is much smaller than at other organic band locations (1660, 1442, and 1200 cm^{-1}). The background could be reduced more accurately due to better signal-to-noise ratio, thus providing the best results. For the purpose of presenting a clear spectrum of the C—H stretching mode for enamel an acquisition time of 72 h was used (Fig. 2). The Labspec V4 software package (Jobin Yvon) was used for peak fitting of the acquired spectra. Peak analysis included (1) maximum peak location, (2) peak intensity, (3) ratio of phosphate band/C—H stretching mode, and (4) ratio of phosphate /carbonate band. A grating groove density of 1800 grooves/mm instead of 600 grooves/mm was used to obtain high-resolution spectra for possible shifts due to different organic material. This was especially necessary for enamel, where the concentration of organic material is small and different proteins than those in dentin can be identified. This automatically narrows the scanning interval down to 1108 to 811 cm^{-1} for the phosphate band and to 3037 to 2842 cm^{-1} for the C—H stretching mode. The scanning interval of the phosphate band includes the carbonate peak at 1070 cm^{-1} . A ratio of the phosphate/carbonate peaks was analyzed based on the relative integrated intensities.

Determination of the width of the DEJ

For the determination of the width of the DEJ three different samples were placed at the focus of a 50 \times microscope objective and spectra were acquired at 1- μm intervals across the DEJ. A 100- μm line perpendicular to the interface was scanned with an acquisition time of 30 s for each measurement. The sample moved in 1- μm intervals across the interface while the laser remained stationary. Lines at three different positions, as shown in Figure 1, were run per sample. Spectra were acquired for the phosphate band in an interval

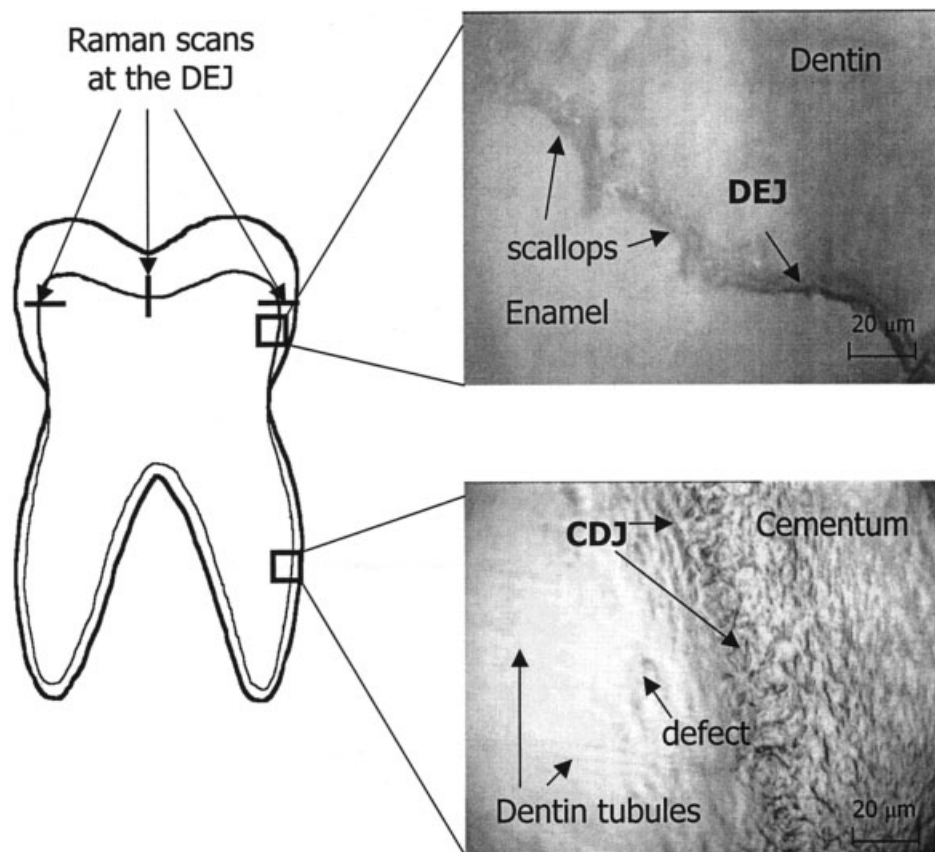


Figure 1. Schematic illustration of the tooth specimen showing areas where Raman spectra were acquired in a perpendicular line across the DEJ and CDJ. The insets show microscopic photos at 50× the DEJ and CDJ.

of 1700 to 600 cm^{-1} and for the C—H stretching mode in an interval of 3300 to 2400 cm^{-1} . The computer program automatically selected these intervals because 600 grooves/mm were used as higher resolution was not needed so a broader range could be sampled. The intensity of the phosphate peak at 960 cm^{-1} was obtained from each measurement. The measurements were then repeated to collect the intensity values for the C—H stretching mode at the position using the band from 3000 to 2850 cm^{-1} , which represents the three peaks of the C—H stretching mode. There was a total of 18 lines (9 for PO_4^{3-} and 9 for C—H measurements). On each sample three lines for PO_4^{3-} and three lines of C—H at different locations were scanned. Each line was 100 μm long and the data were collected in 1- μm steps. Three samples were done this way, resulting in a total of 1800 measurements in the area of the DEJ. The intensity values were plotted as graphs (see Fig. 3). To evaluate the width of the DEJ, linear regression lines were estimated from (1) the data in dentin, (2) the data in enamel, and (3) the slope between dentin and enamel. The intersections of the three regression lines were used to obtain estimates of the DEJ width for each data set, one using the PO_4^{3-} peaks and one using the C—H stretching mode.

In addition to the analysis of the 100- μm lines in different areas of the teeth, the DEJ width was determined from one area of 100 \times 100 μm by scanning in 1- μm steps to see the variation in a small region. A distinct width was calculated for each line of that region, that is, a total of 100 values. The

scan direction was not perpendicular to the DEJ; thus, the measured widths needed to be multiplied by the cosine of the angle between the scan direction and that perpendicular to the DEJ to correct this geometry.

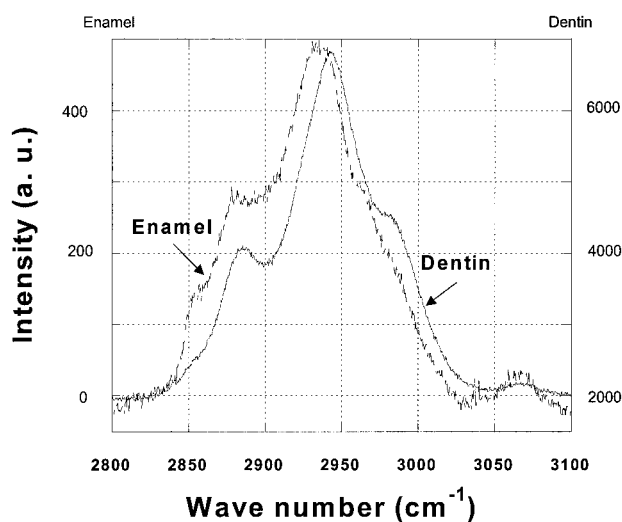


Figure 2. C—H stretching mode for enamel shows a pronounced shift to 2934 cm^{-1} compared to the C—H stretching mode at 2937 cm^{-1} for dentin. Acquisition time for enamel was 72 h and for dentin 600 s.

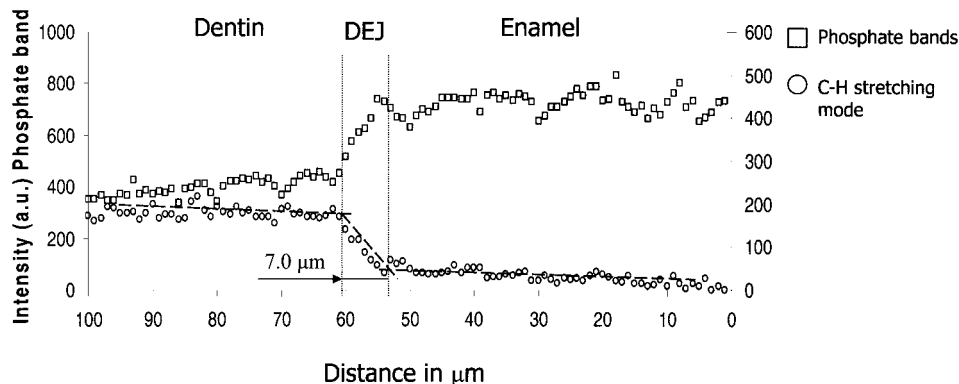


Figure 3. Analysis of a representative course of Raman spectra obtained by scanning perpendicularly across the DEJ in 1- μm steps with an acquisition time of 30 s for a total length of 100 μm . The width of the sloped region relates to the width of the DEJ. Phosphate intensity on left axis, C—H intensity on right axis.

A distribution curve of the estimated widths was plotted for the PO_4^{3-} peaks (total, 100 values) as well as with the C—H stretching mode (total, 100 values).

Statistical methods

A one-way analysis of variance (ANOVA) (SAS statistical software, version 7, SAS Institute, Inc., Cary, NC) and Student–Newman–Keuls test were used to determine statistical significance of compositional differences and confirm peak shifts of the phosphate band at $\approx 960\text{ cm}^{-1}$ and the C—H stretching mode at $\approx 2937\text{ cm}^{-1}$. A Student's *t* test was used to determine any statistical differences between the width of the DEJ using the phosphate band intensity changes and C—H stretching mode changes. Intratooth differences in the width of the DEJ in buccal, lingual, and occlusal regions were evaluated using one-way ANOVA and Student–Newman–Keuls tests.

RESULTS

Compositional analysis of mineralized dental hard tissue

Table I includes high-resolution peak analysis for each of the tissue substrates and junctions: dentin,

DEJ, enamel, CDJ, and cementum. The peaks for the phosphate bands were located for all substrates between 959.5 and 960.2 cm^{-1} . The mean was 959.8 cm^{-1} . No significant differences could be found among the tissues or junctions ($p = 0.47$). The C—H peaks for dentin, CDJ, and cementum were located between 2937.9 and 2938.6 cm^{-1} . A shift of the C—H stretching mode was clearly seen (Fig. 2) for the enamel and the DEJ compared to the dentin C—H stretching mode. The peaks were located at 2934.3 and 2935.7 cm^{-1} and 2938.6 cm^{-1} , respectively. Statistically significant differences at the $p < 0.05$ confidence level among all mineralized tissues with respect to the C—H peak location were found except between cementum and the CDJ ($p = 0.093$) and between cementum and dentin ($p = 0.099$).

The phosphate/C—H ratio clearly showed that enamel had a different average composition than the adjacent hard tissues. The cementum had the lowest (2.8) and enamel the highest ratio (94.2). The phosphate/C—H intensity ratio for dentin was approximately 10% that of enamel. Comparing the phosphate with the carbonate intensities the ratios were similar for dentin, the CDJ, and cementum with 7.1, 6.8, and 6.5, respectively, while for the DEJ and enamel it resulted in 18.7 and 19.6, respectively (Table I). Figure 2 shows the C—H stretching for enamel and dentin

TABLE I
Shift Analysis of Phosphate Band Versus C—H Stretching Mode, Phosphate/C—H Stretching Mode Ratios, and Phosphate/Carbonate Ratios

	Maximum Peak Location (cm^{-1})		Intensity Ratio $\text{PO}_4^{3-}/\text{C—H}$	Intensity Ratio $\text{PO}_4^{3-}/\text{CO}_3^{2-}$
	Phosphate	C—H		
Dentin	959.9 \pm 0.2	2938.9 \pm 0.5	9.9	7.1
DEJ	959.9 \pm 0.4	2935.7 \pm 0.6	10.5	18.7
Enamel	959.6 \pm 0.4	2934.3 \pm 0.3	94.2	19.6
CDJ	959.8 \pm 0.1	2937.4 \pm 0.4	3.3	6.8
Cementum	959.8 \pm 0.5	2938.2 \pm 0.4	2.8	6.5

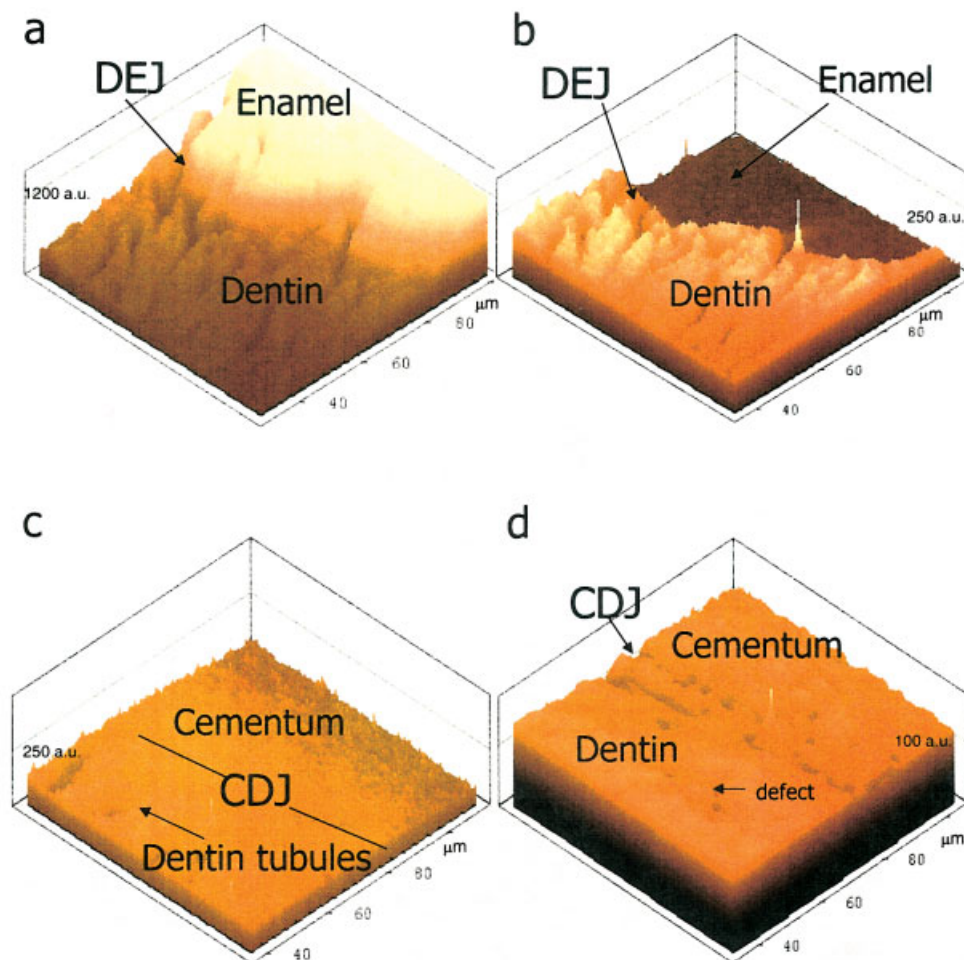


Figure 4. 3D Raman spectroscopic analysis of the areas shown in Figure 1. (a) Scanning DEJ area with respect to phosphate band. (b) Scanning DEJ area with respect to C—H stretching mode. (c) Scanning CDJ area with respect to phosphate band. (d) Scanning CDJ area with respect to C—H stretching mode (defect in collagen is visible and congruent with defect in Fig. 1 CDJ area). [Color figure can be viewed in the online issue, which is available at www.interscience.wiley.com.]

between 3100 and 2800 cm^{-1} . The spectra have two different scales because of different acquisition times. The enamel spectrum shows an additional fourth peak at 2850 cm^{-1} .

Determination of the width of the DEJ

Using the intensity of the phosphate peaks at 959 cm^{-1} , lines across the DEJ yielded a mean width of 7.6 (± 2.8) μm based on the gradient zone. The intensities of the C—H stretching mode and the phosphate band are plotted in Figure 3 for a representative 100- μm line across the DEJ. When using the gradient measurement method for the C—H stretching mode a somewhat wider DEJ was determined, with a mean width of 8.6 (± 3.6) μm . A *t* test showed no significant difference between the two estimates of the width of the DEJ ($p = 0.56$). A one-way ANOVA showed that there were no significant differences in DEJ width at buccal, lingual,

or occlusal locations of the tooth ($p = 0.18$). Figure 4 shows 3D images of the DEJ and CDJ locations with the intensity of phosphate band peaks [Fig. 4(a,c)] or with the C—H stretching mode peaks [Fig. 4(b,d)] in 1- μm steps and an acquisition time of 30 s. The DEJ images show strong intensity differences when scanned with the phosphate band [Fig. 4(a)] or with the C—H band [Fig. 4(b)]. For the area displayed in Figure 4(a,b) width values were determined for 100 lines in the 100 \times 100- μm area, resulting in a distribution curve for the width of the DEJ, as shown in Figure 5. In this graph widths of 7 and 8 μm were most abundant, followed by widths of 4 and 6 μm . The range of values was large, from 1–10 μm . However, the median values of 6 and 7 μm confirmed the findings estimated with single lines in different regions of the tooth.

The images in Figure 4(c,d) suggest that there is no clear distinguishable zone that can be identified as the CDJ. There was no gradient zone as seen between

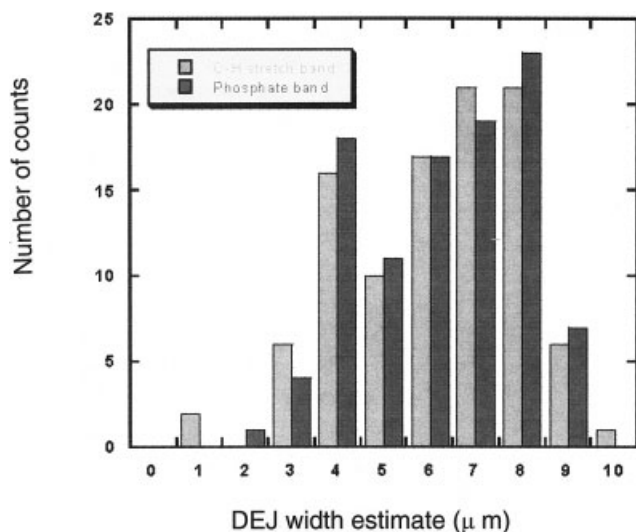


Figure 5. Distribution curve for DEJ width determined with phosphate band peaks and C—H stretching mode peaks.

dentin and enamel. Therefore, the width could not be determined using this gradient zone method. However, a highly fluorescent zone of about 20 to 30 μm was detected at this junction.

Figure 6 displays a 2D total emission image with a resolution of $1 \times 1 \mu\text{m}$ and an acquisition time of 30 s per measurement. After subtracting the fluorescence from the image, no difference could be seen between dentin, CDJ, and cementum, as demonstrated in Figure 4(d).

A shallow valley was present in the intensity plot of the C—H band at each side of the CDJ, as shown in Figure 7 and in the 3D image [Fig. 4(d)].

DISCUSSION

Raman spectroscopy is an advanced, fast analytic technique to determine the structure and chemical composition of materials. It provides chemical information based on molecular vibrations of the molecules in the sample. In this study the spectra from human dental hard tissues were analyzed in two specific wave number locations, the phosphate stretching band and the C—H stretching mode.

Apatite mineral exhibits characteristic spectra in the frequency range from 1700 to 600 cm^{-1} .²¹ The mineral portion of the Raman spectra from all substrates exhibited the characteristics of carbonated hydroxyapatite (HAP) with stronger peaks for the phosphate stretching mode PO_4^{3-} (959 cm^{-1}) than for the carbonate mode CO_3^{2-} at 1072 cm^{-1} . The envelope of the C—H stretching mode (3300 to 2400 cm^{-1}) was used in this study because it had the potential to detect differences in noncollagenous proteins as well as col-

lagen. It is less often investigated as a signature of the organic content in dental hard tissues but has been studied frequently in bone deproteinization analysis, as discussed by Pelletier²¹ and Termine et al.²⁶

The gradient zone between dentin and cementum was difficult to measure because the zone exhibited fluorescence. This may be due to impurities incorporated during sample preparation or to the luminescent nature of proteins, which are more abundant in this area. Further studies need to address this question.

The gradient zone between enamel and dentin seen with the C—H stretching mode is due to the low organic content ($\approx 4\%$) in enamel. No collagen type I is present, but proteins of this matrix include the tyrosine-rich amelogenin polypeptide and other “nonamelogenin” proteins, such as enamelin, tuftelin, ameloblastin, serum albumin, and proteinases, although the origin of the serum proteins is thought to lie in postextraction contamination.^{10,27} The difference between collagen type I in dentin and the organic component of enamel was clear in the shift of the C—H stretching mode with long acquisition time. The enamel spectrum in Figure 2 was obtained with 72 h acquisition time to diminish the noise, while the dentin spectrum required only 600 s. This adjustment was made to better visualize the differences in the two C—H stretching mode locations. The C—H stretching mode usually absorbs near 2890 cm^{-1} , but this band is found in a broader region, 3000 to 2850 cm^{-1} , when the C—H is adjacent to a noncarbon atom.²¹ It is likely that apatite-forming molecules surround the C—H, causing the entire band to shift. Visual examination did not reveal any apparent change in the enamel but prolonged laser exposure may have caused the peak shift.^{28,29} Further studies are necessary to eliminate these possibilities.

This study found pronounced changes in peaks from mineral and organic components, which yielded

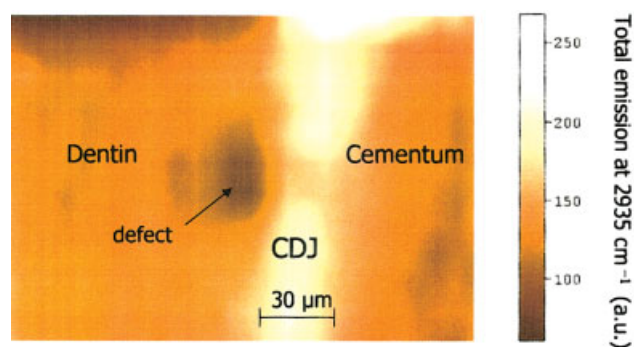


Figure 6. 2D Raman image of the CDJ area. The scanned area shows total emission of the C—H stretching mode only. The image shows a highly fluorescent band of about 30 μm highlighting the CDJ. [Color figure can be viewed in the online issue, which is available at www.interscience.wiley.com.

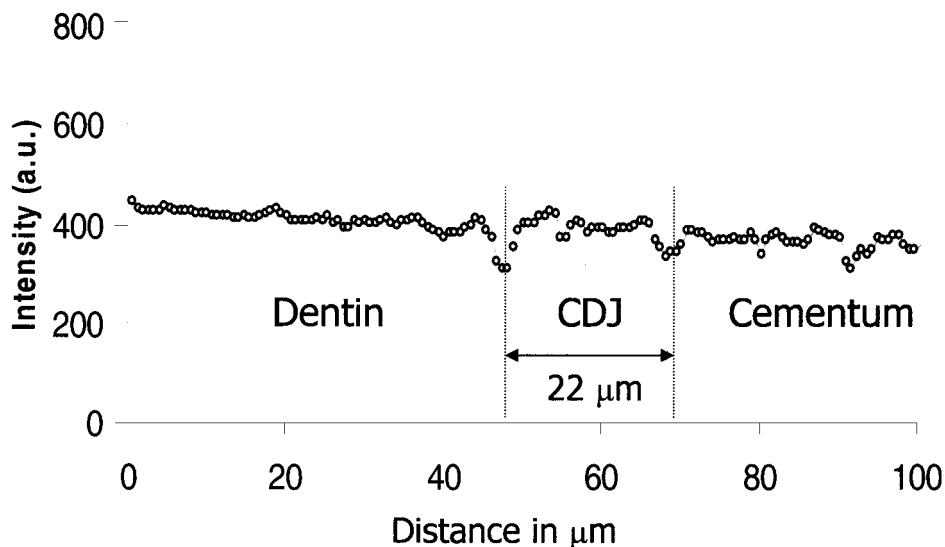


Figure 7. Scanned line of 100 μm across the CDJ using Raman spectroscopy at the C—H stretching mode including the 2882-, 2934-, and 2989- cm^{-1} bands. A shallow valley adjacent to the CDJ marks the CDJ band. This observation was made on several CDJ samples. Figure 3(d) shows these valleys in a 3D image.

information about the connecting zones, such as the DEJ. However, this system has limitations and could not identify a well-differentiated junction between dentin and cementum because the mineral and organic contents are similar. The long acquisition times per measurement point yielded a high-resolution analysis, shown in Table I, with precise maximum peak locations with low standard deviations. The statistically significant differences, found with respect to the peak locations from the C—H mode, between the DEJ, dentin, and enamel may support the hypothesis that the DEJ has a different chemical composition than the adjacent tissues, dentin, and enamel. However, these significant peak shifts might be due to the blending of different organic compounds or due to the differences in composition between the organic contents in dentin³⁰ and noncollagen-type proteins in enamel.³¹ This is likely because the C—H peak from the DEJ was 2935.7 cm^{-1} , between the peaks for dentin and enamel. Whether it is a combination of organic and nonorganic compounds or a new material remains unclear. Therefore, the hypothesis that the DEJ is a separate entity could not be clearly established and it is assumed to be a gradient zone.

No peak shifts between the CDJ and cementum and between cementum and dentin could be seen using the C—H mode. This indicates that the latter materials are composed of similar structures and the hypothesis that the junction has similar composition to cementum and dentin can be verified. Analyzing the peak locations with respect to the PO_4^{3-} band, all substrates showed the same peak location at 959 cm^{-1} . The Raman intensities for both the PO_4^{3-} band and the C—H stretching mode from the DEJ exhibited linear gradient zones, as presented in Figure 3. This suggests that

the concentration of organic and inorganic materials is monotonically changing. The phosphate/C—H ratios demonstrate a ratio difference from 2.8 for cementum to 94.2 for enamel. The phosphate/carbonate ratios varied from 7.1 for dentin to 19.6 for enamel. The value of 18.7 for the DEJ was closer to that of enamel, in contrast to the phosphate/C—H ratios, where the DEJ was similar to dentin. (Table I)

The width of the DEJ has been evaluated based on the morphological structure⁷ as well as mechanical properties. The DEJ functional width was reported as being 27–100 μm wide⁴ using Vickers microhardness measurements. Nanomechanical techniques have yielded a significantly narrower DEJ width. Fong et al.³ reported a DEJ width of 15–25 μm , while Marshall et al.² found 10–13 μm , both using nanoindentation. A nanoscratching method using the atomic force microscope (AFM) measured by Habelitz et al.¹ revealed a narrow transitional zone of 1–3 μm , established with friction properties. The latter can provide improved estimates of mechanical property changes because it continuously measures the friction coefficient. Nano- and microindentations require spacing to avoid interaction of the plastic zones and the contact stress fields. The present study measured the chemical composition in 1- μm steps and with a laser penetration of about 1 μm in depth in the sample. Thus, the micro-Raman data suggests that the DEJ contains no unique chemical component and its characteristics can be explained as a mixture of enamel and dentin. The results in Figure 5 demonstrate that the calculation of the width of the DEJ gives almost the same answer when using the C—H mode or the phosphate band. This study showed that the micro-Raman technique can be used to discriminate between different proteins as in colla-

gen type I in dentin³⁰ and amelogenin or other proteins in enamel.³¹ The specific peak position for collagen type I in dentin was 2938.6 cm⁻¹ and for the protein composition in enamel 2934.3 cm⁻¹.

CONCLUSIONS

Mineralized tissues in the tooth were compared using Raman spectroscopy, showing the DEJ and the CDJ as zones of chemical transition rather than separate phases. The DEJ width yielded similar results to those determined using nanomechanical methods. Also, a peak shift of 4.6 cm⁻¹ was found when comparing organic components of dentin with enamel, revealing that collagen type I molecules in dentin have a different maximum peak position for the C—H stretching mode than the noncollagen proteins in enamel.

References

- Habelitz S, Marshall SJ, Marshall GW Jr., Balooch M. The functional width of the dentino-enamel junction determined by AFM-based nanoscratching. *J Struct Biol* 2001;135:294–301.
- Marshall GW Jr., Balooch M, Gallagher RR, Gansky SA, Marshall SJ. Mechanical properties of the dentinoenamel junction: AFM studies of nanohardness, elastic modulus, and fracture. *J Biomed Mater Res* 2001;54:87–95.
- Fong H, Sarikaya M, White SN, Snead ML. Nano-mechanical properties profiles across dentin-enamel junction of human incisor teeth. *Mat Sci Eng C Biomim Supramol Sys* 2000;C7:119–128.
- White SN, Paine ML, Luo W, Sarikaya M, Fong H, Yu ZK, Li ZC, Snead ML. The dentino-enamel junction is a broad transitional zone uniting dissimilar bioceramic composites. *J Am Ceram Soc* 2000;83:238–240.
- Tramini P, Pelissier B, Valcarcel J, Bonnet B, Maury L. A Raman spectroscopic investigation of dentin and enamel structures modified by lactic acid. *Caries Res* 2000;34:233–240.
- Lin CP, Douglas WH. Structure-property relations and crack resistance at the bovine dentin-enamel junction. *J Dent Res* 1994;73:1072–1078.
- Arsenault AL, Robinson BW. The dentino-enamel junction—a structural and microanalytical study of early mineralization. *Calcif Tissue Int* 1989;45:111–121.
- Brännström M. Dentin and pulp in restorative dentistry. London: Wolfe Medical Publications; 1982. p 125.
- Scott JH, Symons NBB. Introduction to dental anatomy, 6th ed. Edinburgh: Livingstone; 1971. p 448.
- Marshall SJ, Balooch M, Habelitz S, Balooch G, Gallagher R, Marshall GW. The dentin-enamel junction—a natural, multi-level interface. *J Eur Ceram Soc* 2003;23:2897–2904.
- Ten Cate AR. Oral histology: development, structure, and function, 5th ed. St. Louis, MO: Mosby; 1998. p 497.
- Bodecker CFW. The distribution of living matter in human dentin, cement and enamel. *Dent Cosmos* 1957;20:582–590.
- Bencz L. Befunde an der dentinzement grenze. *Z Stomat* 1927;5:877–896.
- Blackwood HJJ. Intermediate cementum. *Br Dent J* 1957;102:345–350.
- Brear K, Currey JD, Pond CM, Ramsay MA. The mechanical properties of the dentine and cement of the tusk of the narwhal *Monodon monoceros* compared with those of other mineralized tissues. *Arch Oral Biol* 1990;35:615–621.
- Habelitz S, Marshall SJ, Marshall GW, Balooch M. Mechanical properties of human dental enamel on the nanometre scale. *Arch Oral Biol* 2001;46:173–183.
- Kinney JH, Balooch M, Marshall GW, Marshall SJ. A micromechanics model of the elastic properties of human dentine. *Arch Oral Biol* 1999;44:813–822.
- Balooch M, Wu-Magidi IC, Balazs A, Lundkvist AS, Marshall SJ, Marshall GW, Siekhaus WJ, Kinney JH. Viscoelastic properties of demineralized human dentin measured in water with atomic force microscope (AFM)-based indentation. *J Biomed Mater Res* 1998;40:539–544.
- Yamamoto T, Domon T, Takahashi S, Islam MN, Suzuki R. The fibrillar structure of the cemento-dentinal junction in different kinds of human teeth. *J Periodont Res* 2001;36:317–321.
- el Mostehy MR, Stallard RE. Intermediate cementum. *J Periodont Res* 1968;3:24–29.
- Pelletier M, Pelletier MJ. Analytical applications of Raman spectroscopy. Malden, MA: Blackwell Science; 1999. p 478.
- Suzuki M, Kato H, Wakumoto S. Vibrational analysis by raman spectroscopy of the interface between dental adhesive resin and dentin. *J Dent Res* 1991;70:1092–1097.
- Lemor RM, Kruger MB, Wieliczka DM, Swafford JR, Spencer P. Spectroscopic and morphologic characterization of the dentin/adhesive interface. *J Biomed Optics* 1999;4:22–27.
- Hendra P, Jones C, Warnes G. Fourier transform Raman spectroscopy: instrumentation and chemical applications. Ellis Horwood series in analytical chemistry. New York: Ellis Horwood; 1991. p 311.
- White JM, Goodis HE, Marshall SJ, Marshall GW. Sterilization of teeth by gamma radiation. *J Dent Res* 1994;73:1560–1567.
- Termine JD, Eanes ED, Greenfield DJ, Nylen MU. Hydrazine-deproteinated bone mineral. *Calc Tissue Res* 1973;12:73–90.
- Chadwick D, Cardew G. Dental enamel. Chiba Foundation symposium. Chichester, UK: Wiley; 1997. p 284.
- Wiekuczja DM, Spencer P, Kruger MB. Raman mapping of the dentin/adhesive interface. *Appl Spectrosc* 1996;50:1500–1504.
- Wieliczka DM, Kruger MB, Spencer P. Raman imaging of dental adhesive diffusion. *Appl Spectrosc* 1997;51:1593–1596.
- Butler WT, Ritchie H. The nature and functional significance of dentin extracellular matrix proteins. *Int J Dev Biol* 1995;39:169–179.
- Robinson C, Brookes SJ, Shore RC, Kirkham J. The developing enamel matrix: nature and function. *Eur J Oral Sci* 1998;106:282–291.